

Capture-Gamma Determination of V^{51} Levels*†

J. E. SCHWÄGER‡

Lawrence Radiation Laboratory, University of California, Livermore, California

(Received July 11, 1960)

A fast-coincidence scintillation spectrometer has been developed for thermal-neutron capture-gamma studies at the Livermore 1-Mw pool-type reactor. The added-neutron binding energy in V^{51} was measured as 11.1 ± 0.1 Mev. Cascade radiations for V^{51*} were observed and a decay scheme is established which verifies a previously proposed (p, p') level scheme. Spin assignments for most of the $V^{51}(p, p')$ reported levels below 4.0 Mev are proposed and the level order for the $(1f_{7/2})^3$ proton configuration levels is established as $7/2^-$ (ground state), $5/2^-$, $3/2^-$, $11/2^-$, $9/2^-$, and $15/2^-$ spin with excitation energies of 0.32, 0.93, 1.61, 1.81, and 2.70 Mev, respectively. Of the various nuclear force assumptions that can be made, the short-range force approximation (δ -type interaction) and weak surface-coupling effects for V^{51*}

configuration states appear to give the best match between theory and experiment. A previous calculation using experimentally measured splittings of the j^2 configuration together with tabulated coefficients of fractional parentage gives excellent agreement with experiment. Evidence is also found for $(1f_{7/2}^2)_0 2p_{3/2}$ - and $(1f_{7/2}^2)_0 1f_{5/2}$ -proton single-particle levels at 2.41 and 2.55 Mev, respectively, as well as for additional low-spin states between 2.70 and 3.38 Mev which possibly represent even states resulting from excitation of a lower shell proton to give a $(1f_{7/2}^4)_0$ configuration plus a proton hole in the vacated shell. Experimental results suggest that the V^{51*} 20–28 core is a more rigid structure than the Ca^{48*} 20–20 core.

INTRODUCTION

THE $(1f_{7/2})^3$ configuration allows six states with spins $3/2$, $5/2$, $7/2$, $9/2$, $11/2$, and $15/2$. If only the potential energy of interaction among $1f_{7/2}$ nucleons splits the levels, the theory of holes assures that the level order for n identical particles is the same as for n identical holes and the $(1f_{7/2})^3$ and $(1f_{7/2})^{-3}$ configurations should have identical behavior. Several authors have made theoretical calculations on level spacing and order for these configurations as functions of the range of various assumed nuclear forces.^{1–7} Experimental evidence needed to check theories for the $(1f_{7/2})^{\pm 3}$ multiplet is best obtained from Ca^{48*} or Ca^{45*} with 20 protons in closed shells and 3 or 5 $(1f_{7/2})$ neutrons, and V^{51*} or Mn^{53*} with 3 or 5 $(1f_{7/2})$ protons and 28 neutrons in closed shells.

We know that Ca^{48} , V^{51} , and Mn^{53} all have a measured ground-state spin of $7/2$ as predicted by the Mayer-Jensen model.^{1,8,9} With a $7/2^-$ ground state, theory clearly indicates spins of $5/2^-$, $3/2^-$, and $15/2^-$ for the first two and last of the possible $(1f_{7/2})^3$ excited states,

respectively, but the predicted spins for the third and fourth configuration states are not unanimous. Calculations by Kurath⁷ suggest only the order $9/2$ and $11/2$ whereas Levinson and Ford^{10,11} as well as Lawson and Uretsky¹² predict the order $11/2$ and $9/2$. Edmonds and Flowers⁶ contribute a happy compromise by finding a crossover which permits either order, depending upon the assumed force range. Kurath makes his predictions for strong spin-orbit coupling with "Majorana plus Bartlett" interaction while Levinson and Ford base their calculations on Ca^{41*} and Ca^{43*} using an additional weak particle-coupling to the nuclear surface. Lawson and Uretsky make use of experimentally measured splittings of the j^2 configuration together with tabulated coefficients of fractional parentage.⁵ Additionally, Nussbaum¹³ indicates that single-particle odd levels should also occur at higher energies in the order $2p_{3/2}$, $1f_{5/2}$, and $2p_{1/2}$.

Previously existing knowledge on the excited states of V^{51*} has come from inelastic scattering experiments and from beta decay of Ti^{51} and Cr^{51} . Although poor agreement occurs for the Ti^{51} beta-decay energy, all experimenters concur on observations of a 0.323-Mev gamma ray.^{9,14} Additionally, Jordan¹⁵ *et al.* and Bunker and Starner^{16,17} report 0.928- and 0.605-Mev gammas, the latter in coincidence with a 0.323-Mev quantum, whereas Schardt and Welker¹⁸ observed singles radiation only at 0.325 and 0.94 Mev. Since the shell model indicates that Ti^{51} should have a $3/2^-$ ground state, these data suggest levels in V^{51*} at 0.323 and 0.93 Mev with $5/2^-$ and $3/2^-$ spins, respectively. Several authors⁹

* Work was performed under auspices of the U. S. Atomic Energy Commission.

† These results are taken from a thesis submitted by the author to the University of California in partial fulfillment of the requirements for the degree of Doctor of Philosophy in Physics.

‡ Commander, U. S. Navy, on special assignment at Lawrence Radiation Laboratory.

¹ Maria G. Mayer, *Elementary Theory of Nuclear Shell Structure* (John Wiley & Sons, Inc., New York, 1955).

² Dieter Kurath, *Phys. Rev.* **80**, 98 (1950).

³ Igal Talmi, *Phys. Rev.* **82**, 101 (1951).

⁴ B. H. Flowers, *Proc. Roy. Soc. (London)* **A210**, 497 (1951).

⁵ A. R. Edmonds and B. H. Flowers, *Proc. Roy. Soc. (London)* **A214**, 515 (1952).

⁶ A. R. Edmonds and B. H. Flowers, *Proc. Roy. Soc. (London)* **A215**, 120 (1952).

⁷ Dieter Kurath, *Phys. Rev.* **91**, 1430 (1953).

⁸ *Nuclear Shell Schemes* compiled by R. N. King, C. L. McGinnis, R. van Lieshout, and K. Way, Atomic Energy Commission Report TID-5300 (U. S. Government Printing Office, Washington 25, D. C., 1955).

⁹ D. Strominger, J. M. Hollander, and G. T. Seaborg, *Revs. Modern Phys.* **30**, 585 (1958).

¹⁰ K. W. Ford and Carl Levinson, *Phys. Rev.* **100**, 1 (1955).

¹¹ Carl Levinson and K. W. Ford, *Phys. Rev.* **100**, 13 (1955).

¹² R. D. Lawson and J. L. Uretsky, *Phys. Rev.* **106**, 1369 (1957).

¹³ R. H. Nussbaum, *Revs. Modern Phys.* **28**, 423 (1956).

¹⁴ All energies in this paper are reported in Mev units.

¹⁵ W. C. Jordan, S. B. Burson, and J. M. LeBlanc, *Phys. Rev.* **96**, 1582 (1954).

¹⁶ M. E. Bunker and J. W. Starner, *Phys. Rev.* **97**, 1272 (1955).

¹⁷ M. E. Bunker and J. W. Starner, *Phys. Rev.* **99**, 1906 (1955).

¹⁸ A. W. Schardt and J. P. Welker, *Phys. Rev.* **99**, 810 (1955).

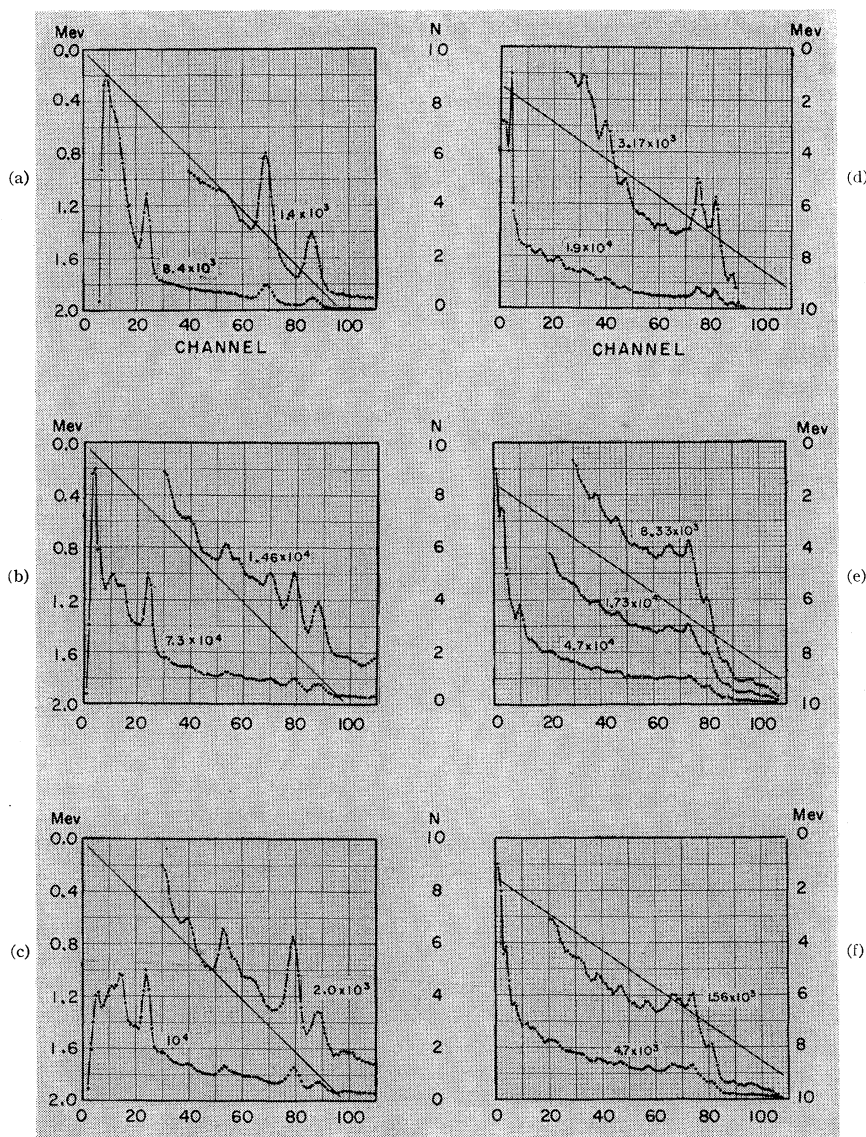


FIG. 1. (a) V^{52} and Al^{28} beta-decay gammas plus reactor background. (b) V^{51*} low-energy singles spectrum. (c) V^{51*} low-energy spectrum in total fast coincidence. (d) Al^{27} capture-gamma total singles spectrum. (e) V^{51*} total singles spectrum. (f) V^{51*} total spectrum in fast coincidence with 0.51 MeV. The number beside the plots is counts per unit of N scale.

report a 0.325-Mev gamma from electron capture of Cr^{51} , while Ofer and Wiener¹⁹ see 0.65- and 0.325-Mev gamma rays, the latter in coincidence with 0.320-Mev thus suggesting a level at 0.65 Mev. Other authors^{20,21} have observed a lower energy quantum which they relate to a possible level at 0.237 or 0.267 Mev.

Several experimenters have employed inelastic proton scattering to study excited states in V^{51*} . Using 8-Mev protons, Hausman *et al.*²² assigned levels at 0.32, 0.48, 1.16, 1.84, 2.22, 2.43, 2.65, 3.11 Mev, and higher

energies, but only the first state agrees with the beta-decay data. Concurrently, Schwäger and Cox²³ observed levels at 0.32, 0.93, and possibly at 0.48 Mev during a limited (p,p') survey for purity of a V^{51} target²⁴ to be used in a $V^{51}(d,p)V^{52}$ reaction. Buechner *et al.*²⁵ completed the work initiated by Schwäger and Cox and reported levels at 0.322, 0.931, 1.609, and 1.819 Mev. Higher levels were observed but could not be assigned because of an intense background. Repeating this work at a later date with the same target, Buechner's group²⁶ was able to remove the background

¹⁹ S. Ofer and R. Wiener, Phys. Rev. **107**, 1639 (1957).

²⁰ H. L. Bradt *et al.*, Helv. Phys. Acta **18**, 259 (1945). See also, however, D. Maeder, P. Preiswerk, and A. Steinemann, Helv. Phys. Acta **25**, 461 (1952).

²¹ B. D. Kern, A. C. G. Mitchell, and D. J. Zaffarano, Phys. Rev. **76**, 94 (1949). See also W. S. Lyon, Phys. Rev. **87**, 1126 (1952).

²² H. J. Hausman *et al.*, Phys. Rev. **88**, 1296 (1952).

²³ J. E. Schwäger and L. A. Cox, thesis, Massachusetts Institute of Technology, 1953 (unpublished).

²⁴ J. E. Schwäger and L. A. Cox, Rev. Sci. Instr. **24**, 986 (1953).

²⁵ W. W. Buechner, C. M. Braams, and A. Sperduto, Phys. Rev. **100**, 1387 (1955).

²⁶ M. Mazari, W. W. Buechner, and A. Sperduto, Phys. Rev. **112**, 1691 (1958).

by better alignment of beam slits and again observed V^{51*} levels at 0.320, 0.930, 1.609, 1.813, plus 31 others at 2.409, 2.545, 2.675, 2.699, 2.790, 3.082 Mev, and higher energies. Coulomb excitation of V^{51} by alpha particles^{27,28} produces gamma rays with energies of 0.33, 0.97, and 1.67 Mev.

Clearly the existing experimental data are conflicting and not adequate to test theory. Consequently, a neutron capture-gamma program was hopefully initiated at the Lawrence Radiation Laboratory (LRL) to help resolve some of the existing controversy and to provide additional data on level spins to check theoretical predictions for this important nucleus. The spectrometer and the experimental procedures developed for its use are discussed in a preceding paper.

SPECTRUM CONTAMINANTS

Vanadium exists almost monoisotopically in nature⁹ as 99.76% V^{51} and only 0.24% V^{50} . Thus it is not surprising that no previous (d,p) or (n,γ) work has been performed with a V^{50} target. The present work was accomplished with 714 mg of V_2O_5 of maximum purity (obtained from Oak Ridge National Laboratory) containing 400 mg of vanadium with 44.1% enrichment of V^{50} irradiated in a 10^5 external thermal neutron beam. Capture cross-section measurements on V^{50} using the pile oscillator technique have not been completed; however, it can be inferred from the capture-gamma experiments that the cross section must be of the order of 100 barns. Since this "precious" sample represented considerable financial liability, it was necessary to provide positive containment even at the risk of handicapping the experiment. Consequently, the sample was tamped into a thin plastic vial, then sealed and encased in a thin-walled aluminum canister. Thus contaminants from Al^{27} , V^{51} , and hydrogen capture gammas²⁹ as well as strong gammas following beta decay of V^{52} and Al^{28} were expected. Figure 1(a) shows the low-energy singles spectrum of the background with V^{50} target in place and reactor "on" but neutron beam "off" (following an immediately prior neutron irradiation) in which the 1.43- and 1.78-Mev beta-decay gammas of V^{52} and Al^{28} are prominent (a check of the decay half-lives verified this identification) as well as a peak from annihilation quanta and an intense lower energy background (always present in reactor experiments). Particular care was taken in the design of collimation and shielding for this experiment with the result that most of the low-energy background comes from high-energy core gammas streaming down the narrow neutron collimator aperture and hitting

the target to form annihilation quanta or Compton scattered radiation. This was demonstrated by beam-off, reactor-on comparative runs with target "in" and "out." Figure 1(b) presents the low-energy V^{51*} -plus-contaminants singles spectrum in which the above-named quanta as well as indications of hydrogen capture radiation appear. Here the 0.51-Mev peak gets additional intensity from high-energy target capture gammas causing pair formation in the crystals and shielding.

One way to clean up the low-energy V^{51*} spectrum is to gate the spectrum with a total fast-coincidence requirement, i.e., only analyze pulses which are in fast coincidence with any other pulse in the spectrum. This is demonstrated in Fig. 1(c) for the low-energy region (the high-energy portion will be discussed later) where it is observed that the 1.43-Mev beta-decay gamma from V^{52} is removed as well as the broad peak in the 2.23-Mev hydrogen capture-gamma region. Equivalently, it can be expected that the 1.78-Mev beta-decay gamma from Al^{28} has also been removed and the remaining peak in the 1.8-Mev region is due to V^{51*} . Coincident annihilation radiation is always present for the facing crystal geometry used because of pair conversion by the target or because of escape annihilation quanta from the other crystal. The coincident annihilation radiation is degraded for 90° angular separation between crystals, but a facing geometry was selected in order to be close to the target. Attention is also invited to the 0.24-Mev coincidence peak which probably originates from 180° Compton backscattering (one crystal to the other for this crystal facing geometry) since it disappears for 90° orientation between crystals. Furthermore, the prominent 0.085-Mev peak in Fig. 1(b) singles spectrum which disappears in the coincidence spectrum can be ascribed to fluorescent radiation from the Pb shielding. Al^{28*} probably causes very weak coincidence peaks at 0.97, 2.11, and 2.27 Mev. Not much contamination is expected from V^{52*} in view of its weak appearance at high energy (to be shown shortly) and the comparatively low intensity of the V^{52} beta-decay peak, but V^{52*} contaminants would occur at 0.13, 0.29, 0.42, 0.65, 0.78, and 0.83 Mev. The 0.13-Mev coincidence peak is prominent whereas only a hint of response exists at 0.42 and 0.65 Mev. The indication at 0.83 Mev is probably too strong to be caused by V^{52*} . None of the remaining prominent coincidence peaks have energies that would attribute them to 180° Compton backscattering for the more intense singles peaks. Consequently the stronger coincidence peaks at 0.32, 0.83, 1.09, 1.18, and 1.30 Mev, and the broad 1.60, 1.79, and 2.02-Mev regions, are tentatively assigned to the V^{51*} spectrum.

A separate survey was made of the Al^{27} capture-capture-gamma spectrum [Fig. 1(d)] which showed

²⁷ G. M. Temmer and N. P. Heydenburg, Phys. Rev. **96**, 426 (1954).

²⁸ V. E. Scherrer, B. A. Allison, and W. R. Faust, Phys. Rev. **96**, 386 (1954).

²⁹ In this paper, radiations specified as "capture gammas" are identified by the parent nuclide whereas excitation radiations refer to the product nuclide of the capture reaction. Thus for $V^{51}(n,\gamma)V^{52*}$, one speaks identically of V^{51} capture gammas or of V^{52*} gammas.

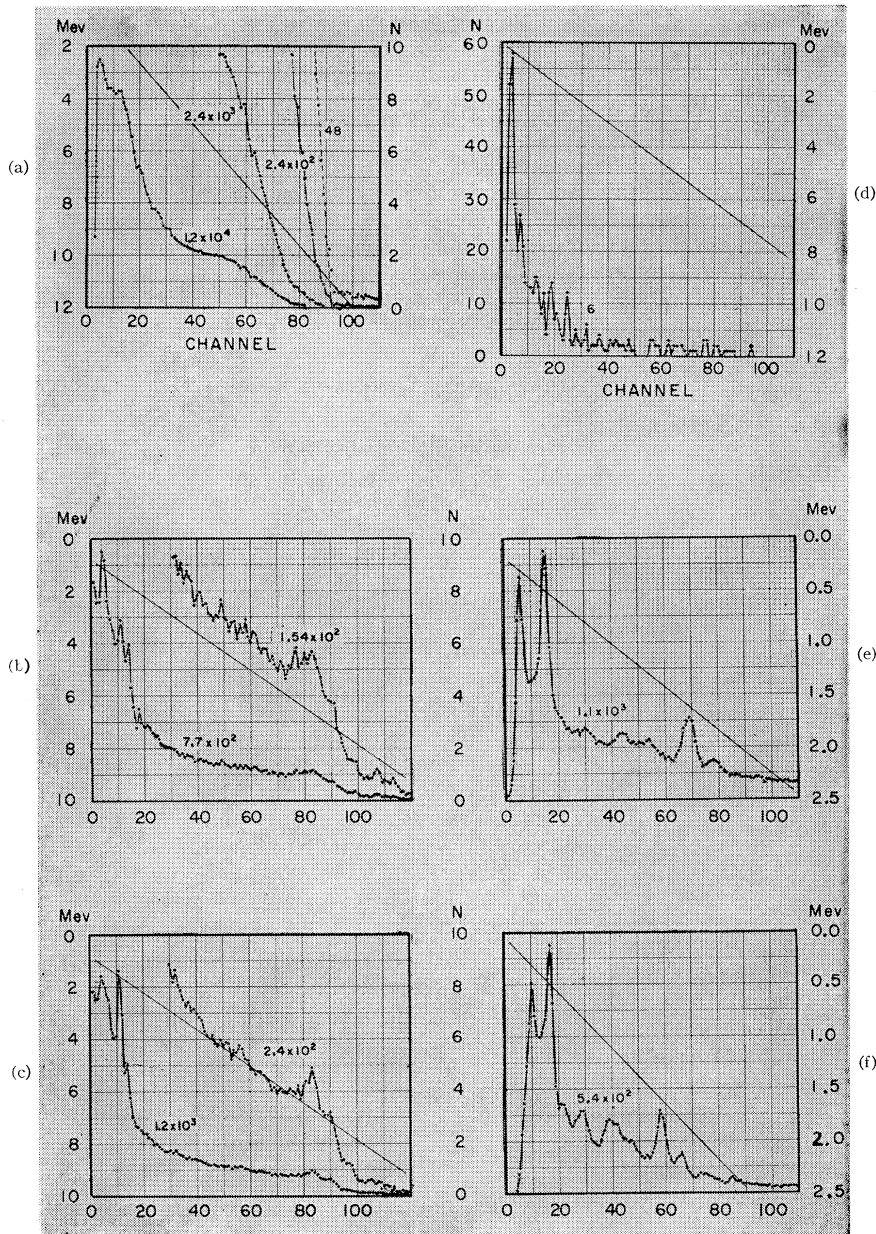


FIG. 2. (a) V^{51*} total sum spectrum in fast coincidence. (b) V^{51*} total spectrum in fast coincidence with 1.6 Mev. (c) V^{51*} total spectrum in fast coincidence with 1.8 Mev. (d) V^{51*} total spectrum in fast coincidence with 1.6 and 1.8 Mev. (e) V^{51*} low-energy spectrum in fast coincidence with 1.8 Mev. (f) V^{51*} low-energy spectrum in fast coincidence with 6.15 to 6.35 Mev. The number beside the plots is counts per units of N scale.

features previously reported by other experimenters.^{30,31} Al^{28*} provides a prominent 7.73-Mev ground-state transition from the capture state (~ 24 photons/100 captures). Thus Fig. 1(d) is of further interest in this paper because it shows the relative intensities of the full energy vs one- and two-escape annihilation peaks at this energy for the 2-in. diam by 2-in. long cylindrical NaI(Tl) crystals used. The crystal faces were placed $\frac{3}{4}$ in. from the target center line at 180° from each other in a plane perpendicular to the 10^5 thermal

³⁰ B. B. Kinsey, G. A. Bartholomew, and W. H. Walker, Phys. Rev. **83**, 519 (1951).

³¹ L. V. Groshev, A. M. Demidov, V. N. Lutsenko, and V. I. Pelekhov, Atomnaya Energ. **3**, 187 (1957).

neutron beam. These peaks were also used for calibration of other high-energy spectrums by stabilizing the system on the always present and prominent 0.51-Mev annihilation peak to prevent gain shifts and then making comparative runs. Calibration of low-energy spectrums was made in an identical manner using various radioactive sources as standards.

The V^{51*} -plus-contaminants singles spectrum reveals indications of radiation up to as high as 9.9 Mev; however, this spectrum is only shown up to 9.0 Mev in Fig. 1(e) because of space limitations. Comparing this spectrum [Fig. 1(e)] with the Al^{28*} singles spectrum [Fig. 1(d)], one sees that except for a prominent peak

at 6.2 Mev and the hint of peaks at 6.0 and 5.5 Mev, the spectrum between 1.8 and 7.7 Mev has the general character of an Al^{28*} contaminant spectrum. Since V^{52*} produces its most intense high-energy radiation at 6.5 Mev with 19 photons/100 captures, it is possible that the 6.0- and 5.5-Mev indications could be the 1- and 2-escape annihilation peaks of V^{52*} 6.5-Mev gammas. The prominent 6.2-Mev peak must be a 2-escape peak from 7.2-Mev radiation because no prominent peak is observed at 5.7 Mev whereas the 6.7- and 7.2-Mev one-escape and full energy peaks could be buried in the intense Al^{28*} peaks of that region. Although V^{52*} has a 7.31-Mev ground-state transition as well as a 7.18-Mev cascade gamma with intensities of 6 and 10 photons/100 captures, respectively, the observed 7.2-Mev radiation is much too intense relative to the identified V^{52*} 6.5-Mev contaminant to be caused by V^{52*} 7.31- or 7.18-Mev radiations. Accordingly, the 6.2-Mev peak is assigned as the 2-escape peak of 7.2 ± 0.05 Mev V^{51*} radiation. These deductions are supported in Fig. 1(f), which shows only one- and two-escape peaks in the high-energy region obtained by gating the fast coincidence spectrum with a 0.51-Mev requirement.

An attempt was made to explore the Al^{28*} peaks for hidden V^{51*} radiation by subtracting contaminants contributed from an identical target holder filled with an equivalent amount of naturally occurring vanadium in the form of V_2O_5 . A series of experiments was made in which varying amounts of the contaminants were subtracted from the initial spectrum and it was found in every case that prominent 6.2, 6.7, 7.2, and 7.7 Mev residual peaks remained. This substantiates assignment of a V^{51*} 7.2-Mev gamma. Furthermore, Bartholomew and Kinsey³² observed weak radiations at 7.67, 7.83, and 7.89 Mev of 0.25, 1.3, and 0.5 photons/100 captures, respectively, as well as a very weak undulation of gammas with higher energies extending up to 9.5 Mev, during their investigation of V^{51} capture gammas (7.31-neutron binding energy) using a V_2O_5 target of naturally occurring vanadium. They concluded (after eliminating the possibility of contaminants) that they had seen high-energy V^{51*} gamma rays following neutron capture in the rare isotope V^{50} . Groshev *et al.*,³¹ however, report they could not detect the alleged V^{51*} gammas even though they examined their natural vanadium capture spectrum with special care in this region. The presently observed indication of a 7.7-Mev residual radiation may well be the 7.67-Mev V^{51*} radiation reported by Bartholomew and Kinsey. If this is true, it is puzzling that the more intense 7.83- and 7.98-Mev V^{51*} quanta assigned by these experimenters do not appear in the present experiment. All indications of responses with energies greater than 7.73 Mev disappear when the target is removed and consequently

³² G. A. Bartholomew and B. B. Kinsey, Phys. Rev. **89**, 386 (1953).

are assigned to V^{51*} radiation. They will be discussed shortly.

EXPERIMENTAL RESULTS

Two measurements^{33,34} of the $V^{51}(\gamma,n)V^{50}$ threshold give a V^{51} neutron binding energy of 10.8 ± 0.5 and 11.15 ± 0.2 Mev, while Johnson³⁵ obtained the value 10.95 ± 0.11 Mev. These data were checked for the present paper (Fig. 2(a)) by electronically summing V^{51*} fast-coincidence cascade radiation. Ignoring the very weak high-energy responses which are probably due to signal pileup, the sum-spectrum asymptotic intersect with the base line at 11.1 ± 0.1 Mev is in good agreement with the previous measurements. Notice also the structure in the sum spectrum at 1.8, 2.7, 3.4, 3.9, 7.2, and 7.7 Mev which suggests prominent cascades from levels represented by these energies.

The measured ground-state spin⁸ of V^{50} is 6, which very likely accounts for its anomalous stability. Both positron and negatron beta decay are energetically possible for V^{50} such that

$${}_{23}V^{50} \rightarrow \beta^+ + {}_{22}Ti^{50} + 2.4 \text{ Mev,}$$

$${}_{23}V^{50} \rightarrow \beta^- + {}_{24}Cr^{50} + 1.2 \text{ Mev,}$$

but neither of these radioactive transitions has yet been detected. A reasonable explanation is that both beta-decay products have zero ground-state spin (even-even nuclei), and a spin change of 6^+ would be a highly forbidden transition. Bauminger and Cohen,³⁶ however, have recently found some positive evidence to indicate that V^{50} decays by K capture to the 1.58 excited state of Ti^{50*} (spin and parity 2^+) with a half-life of $(4.8 \pm 1.2) \times 10^{14}$ yr.

The V^{51*} thermal neutron capture state must have spin and parity $11/2^+$ or $13/2^+$. Since the V^{51} ground-state spin has been established as $7/2^-$,⁸ an 11.1-Mev ground-state transition could occur. The V^{51*} total-singles spectrum only gave indications of weak gammas up to 9.9 Mev, however, and hence a capture to ground-state transition either does not occur or is too weak to be detected in the present experiment.

The observed 0.32, 1.60, and 1.79-Mev V^{51*} radiation (Fig. 1(c)) could correspond to ground-state transitions from corresponding levels previously reported in the (p, p') work. No coincidence peaks were observed at 0.48 Mev (even with the crystals set 90° apart to reduce the 0.51-Mev annihilation coincidence peak) or at 0.93 Mev. Recall that the Ti^{51} and Cr^{51} decay experiments did not show a 0.48-Mev level but did suggest a V^{51*} first level at 0.32 Mev with spin and parity $5/2^-$ and a second level at 0.93 Mev with $3/2^-$. In the present work, observation of 0.32-Mev radiation but none for 0.93 (or 0.48) Mev is

³³ R. Sher, J. Halpern, and W. E. Stephens, Phys. Rev. **81**, 159 (1951).

³⁴ R. Sher, J. Halpern, and A. K. Mann, Phys. Rev. **84**, 387 (1951).

³⁵ W. H. Johnson, Phys. Rev. **87**, 166 (1952).

³⁶ E. R. Bauminger and S. G. Cohen, Phys. Rev. **110**, 953 (1958).

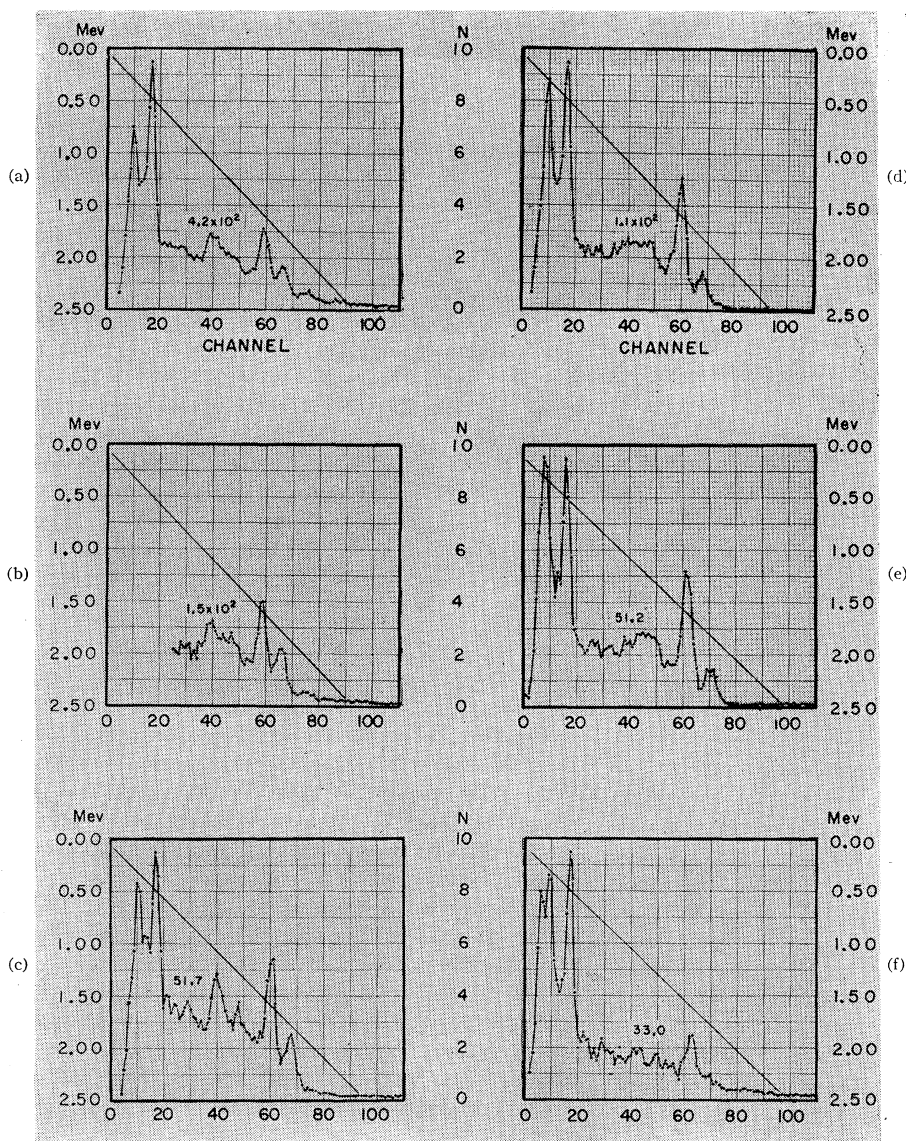


FIG. 3. (a) V^{51*} low-energy spectrum in fast coincidence with 6.65 to 6.85 Mev. (b) V^{51*} low-energy spectrum in fast coincidence with 7.15 to 7.35 Mev. (c) V^{51*} low-energy spectrum in fast coincidence with 7.6 to 7.8 Mev. (d) V^{51*} low-energy spectrum in fast coincidence with 8.25 to 8.35 Mev. (e) V^{51*} low-energy spectrum in fast coincidence with 8.7 to 8.9 Mev. (f) V^{51*} low-energy spectrum in fast coincidence with >9.3 Mev. The number beside the plots is counts per unit of N scale.

also consistent with a $(1f_{7/2})^3$ configuration level order for V^{51*} .

Levels at 1.16 and 2.22 Mev were reported by Hausman *et al.*²² but not observed in the Massachusetts Institute of Technology (MIT) investigations.^{25,26} The intense 1.09-Mev response (Fig. 1(c)) seems too far outside of possible experimental errors to be related to a 1.16 state, but the weaker 1.18-Mev structure is a more likely candidate and will be discussed later. The remaining prominent coincidence radiations (within the energy span being discussed) at 0.83, 1.30, and 2.05 Mev do not correspond to any of the level energies previously reported and may therefore be due to interlevel transitions.

A series of energy-discriminated fast-coincidence experiments showed the 1.60- and 1.79-Mev regions to be in fast coincidence thus suggesting transitions from

a possible 3.39 level to either or both of the 1.60- and 1.79-Mev levels. The width of the responses at 1.60 and 1.79 Mev, however, indicates multiple structure which can be best fitted in the 1.60-Mev region by peaks at 1.57, 1.61, and 1.64 Mev, and by peaks at 1.77, 1.81, and 1.84 Mev in the 1.79-Mev region. Furthermore, experiments with a very narrow discriminator window indicate that 1.81 Mev is separately in fast coincidence with the 1.57-Mev and 1.64-Mev pair and similarly 1.61 Mev is separately in fast coincidence with the 1.77-Mev and 1.84-Mev pair. Accordingly, cascade assignments are tentatively made for transitions from 3.38- and 3.45-Mev levels to both of the 1.61- and 1.81-Mev levels. Since the 1.61-Mev peak is also in coincidence with 0.83, 1.09, 1.18, and the broader 2.02, 2.30, and 2.40-Mev regions, additional cascade assignments are tentatively made for transitions to the 1.61-

Mev level from a 2.70-Mev level and possible multiple levels at 3.6, 3.9, and 4.0 Mev, but an assignment of 0.83 Mev will be temporarily deferred. Although it is within experimental error to speculate that the 0.83-Mev radiation originates from de-excitation of the (p, p') 2.409-Mev level to the 1.609-Mev level, evidence will be presented later to deny this transition. Coincidences were also found between 1.18 Mev and both 1.09 and 1.61 Mev (jointly) indicating that all three are related in cascade. Since ground-state transitions from a substantiated 1.61-Mev level were observed, it seems likely that the 1.18-Mev radiation is derived from a level at 3.88 Mev de-exciting to 2.79 or 2.70 Mev.

The entire spectrum was also examined for fast coincidence with 1.61 and 1.81 Mev (separately) in order to further determine how these levels are populated [Figs. 2(b) and 2(c)]. Details discussed in the previous paragraph are evident in the low-energy region of these experiments, but the high-energy region is difficult to interpret because of multiple (escape) peaks. The general indication is that the 1.61- and 1.81-Mev levels are fed by different transitions, and both are apparently reached from all points of the spectrum. By the nature of the experiment, the region above 6 Mev is free from Al^{28*} and V^{52*} contaminants and should be given particular attention. One distinctive general difference between the spectra is that the 1.61-Mev level is fed by relatively more very high-energy transitions (>8 Mev) than is the 1.81-Mev level, and it appears that 7.2, 7.5, 7.7, 8.8, 9.1, and 9.4-Mev radiations are in coincidence with 1.61 Mev. Another distinction is the relatively strong coincidence between 7.7 and 1.81 Mev. It is within experimental error to postulate a cascade from the capture state to the 3.38-Mev region from which, as determined earlier, de-excitations take place to both the 1.61- and 1.81-Mev levels. A triple-coincidence experiment was performed (three scintillation detectors oriented 90° apart in the same plane) to see what is in fast coincidence with the $3.38 > 1.61$ or 1.81 Mev cascades [Fig. 2(d)]. After 22 hours running time, several peaks appear to be forming in the region below 2 Mev. Nothing definitive can be observed in the higher energy region except that no responses were received above the isolated indication at 7.2 Mev which could be the 1-escape peak from 7.7-Mev radiation. In Fig. 2(e), however, the V^{51*} low-energy spectrum in fast coincidence with 1.8 Mev gammas shows a prominent peak at 1.6-Mev thus demonstrating transitions from the 3.38 and 3.45 Mev levels to the 1.61 Mev level.

In order to improve the high-energy singles-spectrum display, the coincidence spectrometer with 180° crystal separation (i.e., facing geometry) was converted into a two-crystal pair spectrometer by gating with the annihilation peak from one detector and analyzing the spectrum of the other with a fast-coincidence requirement. Thus annihilation quanta escaping from one crystal and being detected in the other will record only

one- or two-escape high-energy peaks. A systematic analysis of this region [Fig. 1(f)] indicates V^{51*} radiation with 7.2, 7.5, 7.7, 8.4, 8.8, 9.3, 9.5, and 9.8-Mev energies.

For additional data to help clarify the decay scheme, fast coincidences were also triggered from various points of interest in the high-energy region (Figs. 2(f)-3(f)). Referring again to the Al^{28*} singles spectrum (Fig. 1(d)), it is evident that coincidence scintillation data obtained in this way requires special interpretation. Since any pulse falling within the window setting will trigger the differential discriminator, gates will be obtained from the Compton tails or escape peaks of any higher energy pulses as well as from full energy peaks at the discriminator setting. Consequently the displays are somewhat subtle in that coincidences with full energy peaks (the information sought) are superimposed on top of a background from higher energy coincidences. For the crystals and geometry of these experiments, Fig. 1(d) shows that triggering will be predominantly from one- and two-escape peaks. In practice, duplicate runs are made with the discriminator set in the valley immediately above the peak being investigated (if a peak exists) to get comparative information for interpretation. An excellent solution for high-energy triggering experiments is to use a three-crystal pair spectrometer for this purpose. Such a spectrometer was built at LRL but the extreme spectrum stability needed (lower coincidence efficiency requires longer data runs) was not attained in time to use the apparatus with the coincidence spectrometer for the data presented in this paper.

Several cascades become apparent by analyzing Figs. 2(f)-3(f) in sequence. As a shorthand aid for the following discussion, energies are understood to be in Mev and the level transitions will be denoted by $A(A-B)B$, where level A de-excites to level B with the release of $(A-B)$ radiation.

(a) **4.00(2.39)1.61**. The 2.39-Mev radiation apparent in Figs. 2(f) and 3(a) disappears in the remainder of the sequence thus indicating that for discriminator settings >7.2 Mev the 4.00-Mev level is no longer populated.

(b) **3.92(2.31)1.61**. The 2.31-Mev relative intensity decreases with increasing discriminator settings and disappears for >7.2 -Mev triggering.

(c) **3.88(1.18)2.70 and 3.88(2.07)1.81**. Observe the mutual weakening of 1.18 and 2.07 Mev in the sequence of Figs. 2(f), 3(a), and 3(b), and finally its disappearance for >7.2 -Mev discriminator settings.

(d) **2.70(1.09)1.61**. The 1.09-Mev response disappears as the discriminator is set >8.3 Mev, thus showing that the 2.70-Mev level is no longer being populated.

(e) **No 2.41(0.60)1.81 or 2.41(0.80)1.61**. If these transitions exist, neither 0.60- or 0.80-Mev-gammas should appear for >8.7 -Mev triggering. Thus the appearance of this radiation in Figs. 3(e) and 3(f) denies that they originate from de-excitation of a 2.41 Mev level.

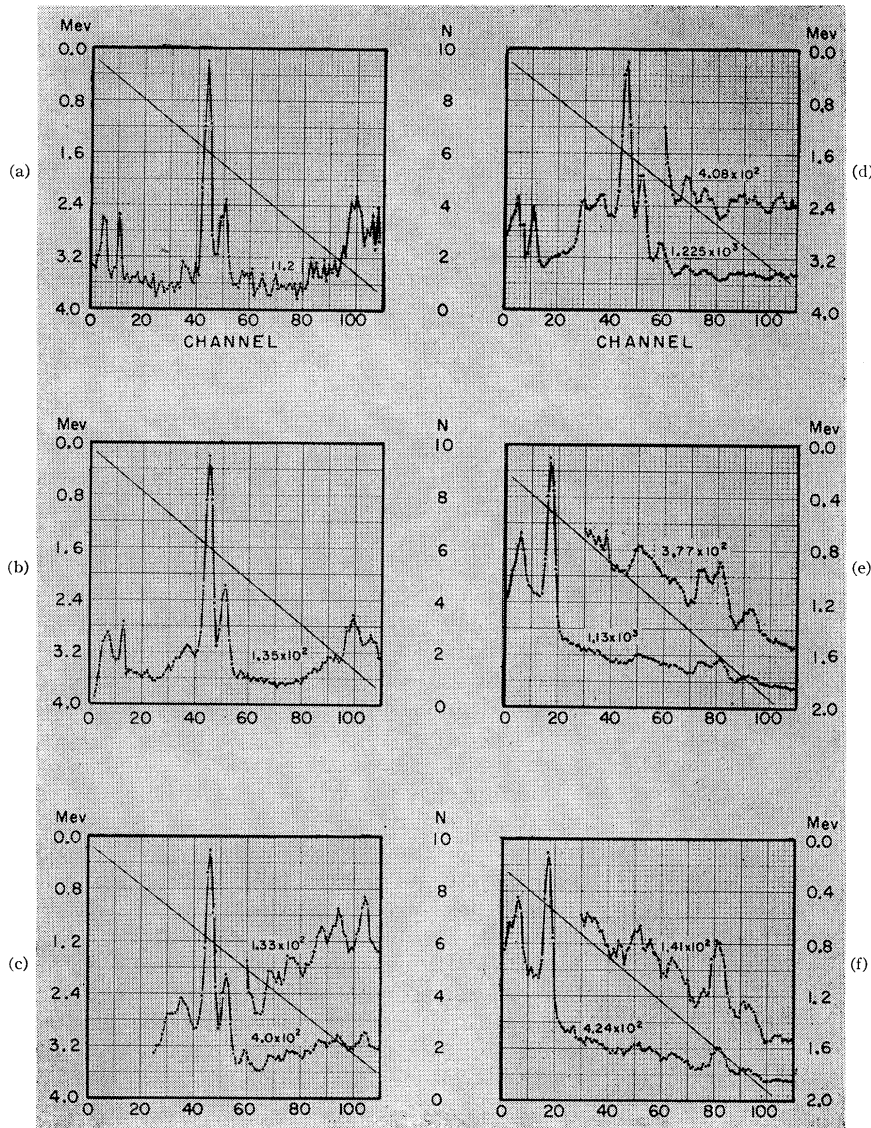


FIG. 4. (a) V^{51*} low-energy spectrum in fast coincidence and sum >10.5 Mev. (b) V^{51*} low-energy spectrum in fast coincidence and sum >10.0 Mev. (c) V^{51*} low-energy spectrum in fast coincidence and sum >9.15 Mev. (1.2 in the ordinate should read 1.6.) (d) V^{51*} low-energy spectrum in fast coincidence and sum >8.1 Mev. (e) V^{51*} low-energy spectrum in fast coincidence with 0.32 Mev. (f) V^{51*} low-energy spectrum in fast coincidence with 0.40 Mev. The number beside the plots is counts per unit of N scale.

All of the level assignments made here correlate with the (p, p') levels reported by the MIT group.^{26,26} Other coincidence radiations appear (notice particularly those at 0.39, 0.44, and the region of 0.6, 0.8, 1.25, and 1.30 Mev), however, which can not be explained by transitions between the low-lying (p, p') levels and would require the introduction of several additional low-energy states to which no other transitions are observed. An alternate and more plausible explanation is that these radiations originate between higher levels in multiple cascades and are likely caused by initial small energy jumps from the capture state (high level density) to adjacent states of lower spin and then to the ground state or to the reported (p, p') states. This situation would also help account for the prominence of the 0.32-Mev peak for high-energy triggering, particularly in Fig. 3(f) where triggering is by >9.3 -

Mev radiation and the 0.32-Mev level could be populated by direct transitions from levels >9.6 Mev following small jumps from the capture state.

Additional level-structure data is obtained with the Hoogenboom sum-coincidence technique³⁷ for detecting double cascades. Unfortunately this method was not workable with the sum-discriminator window positioned for the 11.1-Mev binding energy (negligible photo peaks for high-energy radiation) and it was necessary to use an integral setting triggered by all pulses with sums between the discriminator base line and the binding energy. Figures 4(a)–4(d) show in sequence a series of experiments in which gating was initiated for sums >8.1 through >10.5 Mev and consequently are free from Al^{28*} and V^{52*} radiations. Peaks in these sum-coincidence spectrums are expected to have

³⁷ A. M. Hoogenboom, Nuclear Instr. 3, 57 (1958).

Compton-like tails with length approaching the discriminator window width and to also originate from escape peaks or multiple cascades. Only the lower spectrum is presented (the upper is a mirror image).

Although the statistics are poor for the experiment with sums >10.5 Mev [negligible counting rate; Fig. 4(a)] responses are evident at 0.32, 0.51 (escape annihilation quanta), 1.61, 1.8, 3.38, 3.45, 3.63, and 3.9 Mev which correlate with levels previously deduced. A more practical counting rate was obtained with sums >10.0 Mev [Fig. 4(b)], which verifies these indications. Here the Compton-like tail can be seen below the 1.6- and 3.4-Mev peaks; however, the buildup at 3.1 Mev appears to be somewhat stronger than would be expected from the tail alone. It is possible that this response is augmented by gammas originating from the 3.45-Mev level and de-exciting to the 0.32-Mev level as well as the ground state.

Indicated intensities must be converted to true intensities (by correcting for crystal efficiency, photo-fraction, and peak width) in order to make intensity comparisons. This correction shows the 1.61-Mev peak to be still the most intense; however, the 3.4-Mev region intensity does not appear to be very much weaker. It is difficult to give a reliable quantitative intensity comparison between the peaks because of the poor statistics; however, the situation is much better for the 1.81-Mev response which is 0.6 times the intensity of the 1.61-Mev peak. Since the capture-state spin and parity must be $11/2^+$ or $13/2^+$ and the ground-state spin is $7/2^-$, strong transitions can be expected from the capture state down to lower levels with spins between $9/2$ and $15/2$. Furthermore, ground-state transitions from intermediate levels with spins $>11/2$ are probably negligible if lower levels exist with spins $9/2$ or $11/2$. Consequently, double cascades observed in these sum-coincidence experiments can be expected primarily to reveal spin $9/2$ and $11/2$ levels and allow the important conclusion that the 1.61- and 1.81-Mev levels are the third and fourth high-spin levels of the $(1f_{7/2})^3$ proton configuration states. Additionally, spins $11/2^-$ and $9/2^-$ are tentatively assigned to the 1.61- and 1.81-Mev levels, respectively, because the spin $11/2$ state is probably more highly populated by capture transitions.

There is now also accumulated evidence that the 2.70-Mev level which does not respond in the sum-coincidence spectrum (hence spin $<7/2$ or $>11/2$) is the $(1f_{7/2})^3_{15/2^-}$ proton configuration state. Indications were shown earlier for a strong 2.70(1.09)1.61 transition but no 2.70(0.89)1.81 de-excitation was observed. This would be expected if the 2.70-Mev level spin were $15/2^-$ and the spins of the 1.61- and 1.81-Mev levels were $11/2^-$ and $9/2^-$, respectively. Furthermore, the 3.87-Mev level seems to appear in the sum-coincidence spectrum (hence spin $9/2$ or $11/2$) and coincidence indications were observed for 3.87(1.17)2.70, 3.87(2.06)1.81, and 3.87(2.26)1.61 transitions which would most

probably occur for the tentative spin assignments if the 3.87-Mev level had spin $11/2$. The remaining levels at 3.38, 3.45, and 3.63 Mev could have spin either $9/2$ or $11/2$, but it is not possible at this point to be more specific. Additionally, the other (p, p') levels between 1.81 and 3.38 Mev can be expected to have spins $>11/2$ or $<7/2$ since they do not occur in these sum-coincidence experiments, and more than likely their spins are $<7/2$ because no coincidence transitions were observed from the 2.70-Mev level (spin $15/2^-$) or to the 1.61- or 1.81-Mev levels (spins $11/2^-$ and $9/2^-$).

Several points of interest occur when the discriminator is set to trigger on pulses with sums >9.1 Mev (Fig. 4(c)). Responses which now begin to occur (but which were absent for the higher discriminator settings) must correspond to escape peaks for the previously observed double cascades or be related to multiple cascades for which any two transitions of the sequence have >9.1 -Mev sum. Thus signals are expected (and indications observed) for 2.70(1.09)1.61, 3.63(2.02)1.61, 3.87(2.06)1.81, and 3.92(2.31)1.61 transitions. Notice the buildup at 3.13 Mev which suggests that the earlier-conjectured 3.45(3.13)0.32 transition does occur and consequently the 3.45-Mev level must have a $9/2$ spin. All of these inferences are further substantiated in the next experiment for sums >8.1 Mev [Fig. 4(d)], and previous hints of other formations now become clearly evident. Here a strong response has developed at 2.54 Mev which has the correct energy for a ground-state transition from the (p, p') 2.545-Mev level and, if correct, would have to be related to a multiple cascade for which short jumps occur at higher excitations. This behavior might happen if the last level of the cascade were a low-spin state. By previous conclusion, this level would have $<7/2$ spin and should consequently show de-excitation to the 0.32- or 0.93-Mev level (spins $5/2^-$ and $3/2^-$) as well as to the ground state and will be checked shortly. Furthermore, single-particle proton states in the order of $2p_{3/2^-}$, $1f_{5/2^-}$, and $2p_{1/2^-}$ should begin appear at about these energies³² and according to shell model interpretations^{1,38} the $2p_{3/2^-}$ and $1f_{5/2^-}$ states would be very close together. Accordingly, there is evidence to suggest that the 2.409-Mev level is a $(1f_{7/2^-})^2(2p_{3/2^-})$ proton state and the 2.545 level is a $(1f_{7/2^-})^2(1f_{5/2^-})$ proton state.

There is no reliable evidence to show that the (p, p') levels between 2.70 and 3.38 are populated. By default this suggests they have spins $<7/2$ in concurrence with the sum-coincidence deductions. It is interesting to note that high-energy even states with low spins can occur if a proton from a lower shell is excited to give a $(1f_{7/2^-})^4_0$ configuration plus a proton hole in the vacated shell. If there are no inversions in level order, these states would appear in the inverse order of their observed filling of the states in the previous shell

³⁸ Hisashi Horie and Akito Arima, Phys. Rev. **99**, 778 (1955).

($1d_{3/2}^+$, $2s_{1/2}^+$, $1d_{5/2}^+$) thus giving excitations with spins and parities in the order $3/2^+$, $1/2^+$, and $5/2^+$.

Assignment of spin $11/2$ and $9/2$, respectively, to the 1.61- and 1.81-Mev levels by intensity arguments alone is risky particularly since experimental evidence was shown to suggest that these levels are also being fed by multiple cascades involving small energy changes near the capture state as well as by direct transitions. One way to test the spin assignments is to look for a transition from these levels to the 0.32-Mev level to identify the $9/2$ state. Figure 4(e) (V^{51} low spectrum in fast coincidence with 0.32 Mev) clearly shows a response at 1.49 Mev. As further proof of this transition, the spectrometer discriminator was positioned at 0.40 Mev in the valley above the 0.32-Mev response [Fig. 4(f)] for which the 1.49-Mev indication disappears from the fast-coincidence spectrum. Thus there is strong evidence to support the spin assignments for these levels.

Coincidences between 0.32 Mev and higher levels also gave responses at 2.22 and 3.13 Mev to indicate $2.54(2.22)0.32$ and $3.45(3.13)0.32$ transitions. This is in agreement with the $5/2$ and $9/2$ spins suggested earlier for the 2.54- and 3.45-Mev levels, respectively. Furthermore, the lack of coincidence between 0.32 and 3.06 Mev indicates that the 3.38-Mev level may have $11/2$ spin. The remaining unassigned levels above 3.45 Mev reported in this paper appear to have $9/2$ or $11/2$ spin.

CONCLUSIONS

Conclusions about V^{51*} levels based upon the experimental evidence just presented are summarized in Fig. 5 using the level scheme suggested in reference 26. It is both appropriate and interesting to compare these results with relevant theory and related nuclei.

Kurath⁷ made theoretical calculations for the $(1f_{7/2})^3$ configuration level order and energies using strong spin-orbit coupling with "Majorana plus Bartlett" interaction and no surface effects. This produced an excitation level order with spins $5/2$, $3/2$, $9/2$, $11/2$, and $15/2$ (for all force ranges associated with a $7/2$ ground state) which now conflicts with experimental spins of $11/2$ and $9/2$, respectively, for the third and fourth V^{51} configuration states. Furthermore, the theoretical level spacing does not seem to fit the remaining V^{51*} data when assumptions of various spin misassignments are made. On the other hand, calculations by Edmonds and Flowers^{5,6} for short-range forces are in agreement with this experimental level order but do not match the observed level energies. It is also interesting that an extensive calculation by Hitchcock³⁹ for the V^{50} ground state provides a correct spin of 6 in the short-range approximation (δ -type interaction) whereas a spin of 5 results for forces of the "expected" range. As pointed out by Edmonds and Flowers, the distinction between Majorana and Wigner forces as

well as Bartlett and Heisenberg forces disappears if they have vanishing range. Bohr and Mottelson⁴⁰ have discussed the effects of surface coupling on the j^3 configurations, and very promising results with a weak coupling approximation have been obtained in calculations for a predicted level scheme of Ca^{43*} by Ford and Levinson.^{10,11} The latter authors have shown that weak surface interaction can depress the higher spin states to give a level order which is now observed for V^{51*} . Their calculations for Ca^{43*} , however, were based on an earlier single-particle level-structure assumption for Ca^{41*} which now appears to warrant revision.¹³ Furthermore, the calculations were normalized to fit a Ca^{43*} level scheme proposed by Lindqvist and Mitchell⁴¹⁻⁴³ assigning an expected $9/2^-$ level at 0.81 Mev for which there is now some doubt.^{44,45} Lindqvist and Mitchell point out that the exact agreement of theory with their observations is to be expected since three parameters were used to fit three levels, and a proper test of the theory would be attained if the two unobserved $11/2$ and $15/2$ states were to be found. Determination of these levels and adjustment of the theory to revised calcium data as well as similar calculations for V^{51*} would appear to be very profitable.

Goldstein and Talmi⁴⁶ have suggested that an application of experimentally measured splittings of the j^2 configuration plus tabulated coefficients of fractional parentage⁵ can often make it possible to determine the excitation energies of a j^n configuration. Using this technique, Lawson and Uretsky¹² computed the level order and energy splittings for the $(1f_{7/2})^{-3}$ configuration based on measurements⁴⁷ of the $(1f_{7/2})^{-2}$ configuration for Fe^{54*} . These calculations should also apply to the $(1f_{7/2})^3$ configuration of V^{51*} . Their results predict level order in exact agreement with the present experiment and, with the possible exception of the $15/2^-$ level, provide level spacing which is very close to the observed spacing.

Observations by Bartholomew and Kinsey³² of three possible V^{51*} gamma rays representing capture transitions to ~ 3.4 -Mev levels rightfully led to early conjectures that they were high-spin configuration states. The present experiments confirm the high-spin character of these levels, but the configuration states appear to be at much lower energies ($\sim 1/2$). Reliable data needed on the comparable Ca^{43*} states may be difficult to obtain. Unfortunately a proposed⁴¹⁻⁴³ Ca^{43*} $9/2^-$ level at 0.81 Mev does not appear in the (d,p) work,⁴⁴ but

⁴⁰ A. Bohr and B. R. Mottelson, Kgl. Danske Videnskab, Selskab, Mat.-fys. Medd. **27**, No. 16 (1953).

⁴¹ T. Lindqvist and A. C. G. Mitchell, Phys. Rev. **95**, 444 (1954).

⁴² T. Lindqvist and A. C. G. Mitchell, Phys. Rev. **95**, 612 (1954).

⁴³ T. Lindqvist and A. C. G. Mitchell, Phys. Rev. **95**, 1535 (1954).

⁴⁴ C. M. Braams, Phys. Rev. **95**, 650 (1954).

⁴⁵ C. M. Braams, *Energy Levels of Calcium Isotopes*, thesis (Excelsior, Oranjeplein 96, The Hague, The Netherlands, 1956).

⁴⁶ S. Goldstein and I. Talmi, Phys. Rev. **102**, 589 (1956).

⁴⁷ W. W. Buechner and A. Sperduto, Bull. Am. Phys. Soc. **1**, 39 (1956).

³⁹ A. Hitchcock, Phys. Rev. **87**, 664 (1952).

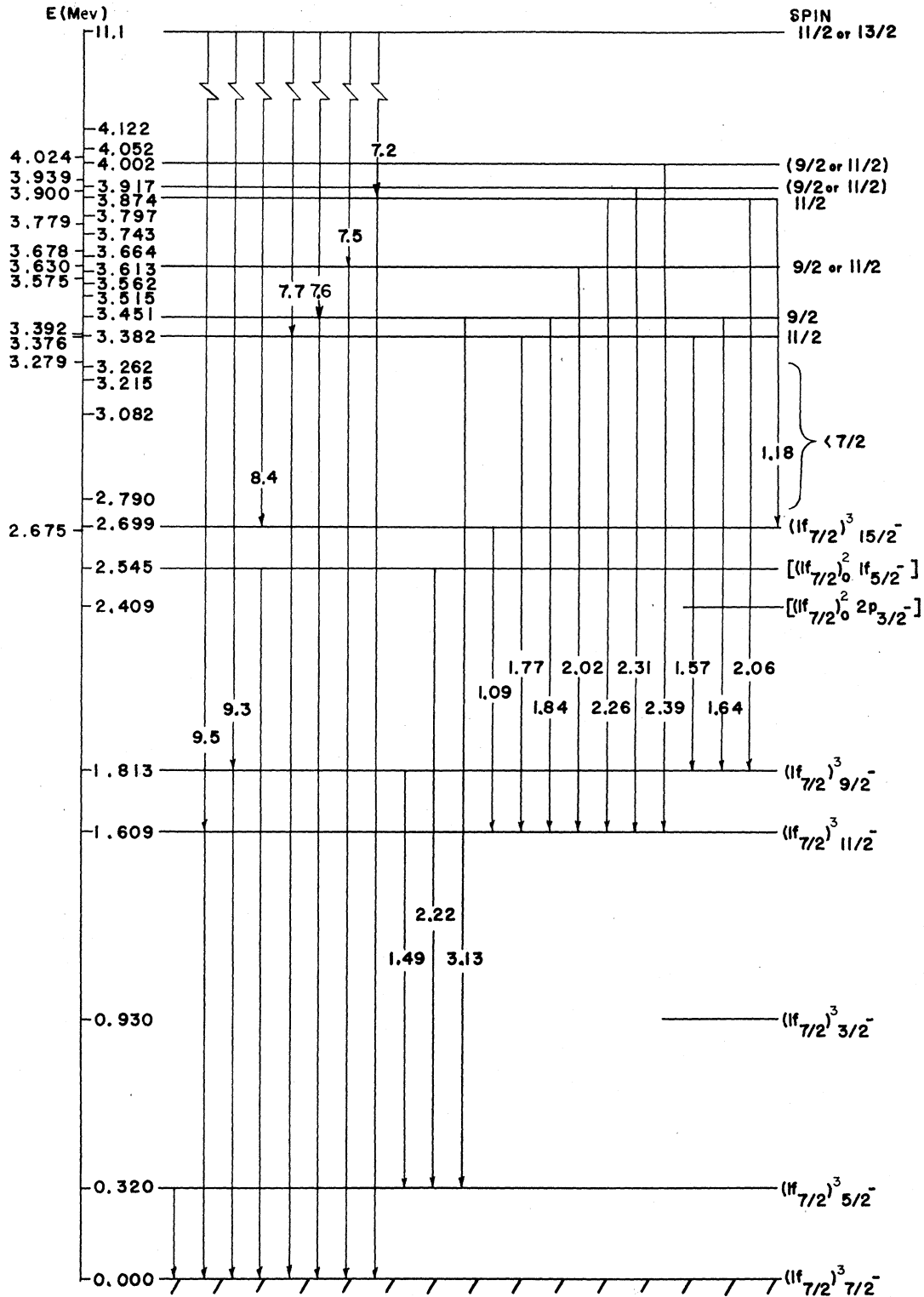


FIG. 5. Gamma-ray decay in ^{51}V .

evidence was found by Braams⁴⁵ for a Ca^{43*} high-spin level at 1.678 Mev. Judging by the energies of the accepted $5/2^-$ and $3/2^-$ Ca^{43*} ($1f_{7/2}$)³ levels, the V^{51*} 20–28 core may be more rigid than the 20–20 Ca^{43*} structure thus indicating that the high-spin Ca^{43*} configuration levels should appear at lower energies than the comparable V^{51*} levels. Other supporting evidence for a tighter core is the possible higher excitation energy in V^{51*} for the $2p_{3/2}$ single-particle level plus even levels (representing breakup of the 20-proton shell core) that are low-lying in Ca^{41*} and Ca^{43*} vs apparently high-lying in V^{51*} . This conclusion is also suggested by the greater excitation energy of Ca^{48*} vs Ca^{40*} or the difference⁸ in Ca^{41*} and Sc^{41*} excitation energies from those of Ca^{49*} and Sc^{49*} .

If the tentatively assigned $15/2$ level at 2.70 Mev exists, one wonders whether it corresponds to the (p, p') 2.675- and 2.699-Mev doublet (angular momentum high for excitation). It would be useful to perform angular distribution measurements with stripping reactions on a V^{50} target to help distinguish between single particle (seniority $s=1$) and mixed V^{51*} states ($s>1$). Definite assignments might be possible from

such (d, p) work to check the tentative proposals of the present work. Schwäger and Cox²⁴ developed a technique for preparing thin vanadium targets requiring a minimum amount of mother material which should help produce appropriate V^{50} targets from a very limited amount of the enriched isotope. This would also permit (p, p') investigations of V^{50*} levels thus giving data on the coupling between $(1f_{7/2})^3$ proton configurations and a $(1f_{7/2})^{-1}$ neutron hole.

ACKNOWLEDGMENTS

I wish to thank Professor Burton J. Moyer for his guidance during the course of this work. The help of Dr. Laurence Passell and Dr. Harry West during the initial development of the spectrometer is profoundly appreciated. Transcending these acknowledgments, I am indebted to Dr. Edward Teller, Dr. Herbert York, Dr. Albert Kirschbaum, and Dr. James Carothers for encouraging and generously supporting the experimental program and to Vice Admiral John T. Hayward, U. S. Navy, Rear Admiral Frederick L. Ashworth, U. S. Navy, and Professor Leonard B. Loeb who have motivated my interest in science.

Elastic Scattering of Alpha Particles from Helium†

J. R. DUNNING, A. M. SMITH, AND F. E. STEIGERT
Yale University, New Haven, Connecticut

(Received September 9, 1960)

The elastic scattering of alpha particles from helium has been investigated at laboratory energies of 6.43, 6.84, and 7.78 Mev. Complete angular distributions from 20° to 90° in the center-of-mass system were obtained. Analysis of the data suggests somewhat smaller values for the D -wave phase shift than previously reported.

INTRODUCTION

THE elastic scattering of alpha particles from helium has been frequently studied in an attempt to better understand the structure of Be^8 . The lower energy data have been quite completely reviewed in the work of Nilson, Jentschke, *et al.*¹ and more recently of Jones, Phillips, and Miller.² The energy region from 4 to 8 Mev (laboratory) is of particular interest in terms of extracting parameters relative to the quite broad first excited state in Be^8 at about 3 Mev. Utilizing the excitation curves at three judiciously chosen angles, specifically the zeros of the second and fourth order Legendre polynomials, Jones *et al.* have investigated this state in

terms of a single-level dispersion theory. As is to be expected, the parameters obtained would appear to be a rather sensitive function of the D -wave phase shifts selected. Specifically, the use of somewhat smaller values than those chosen would tend to decrease the reduced width of the state and to increase the accompanying hard sphere radius. Such a lowering is indeed implied by an extrapolation of Nilson's data into this energy region. The data of Berk, Steigert, and Salinger³ would likewise seem to support somewhat smaller values.

The various attempts to connect the experimental phase shifts with theoretical potentials are briefly reviewed by Butcher and McNamee.⁴ Utilizing a force law combination observed to give good results in esti-

† This work was performed under the auspices of the Office of Naval Research.

¹ R. Nilson, W. K. Jentschke, G. R. Briggs, R. O. Kerman, and J. N. Snyder, *Phys. Rev.* **109**, 850 (1958).

² C. M. Jones, G. C. Phillips, and P. D. Miller, *Phys. Rev.* **117**, 525 (1960).

³ N. Berk, F. E. Steigert, and G. L. Salinger, *Phys. Rev.* **117**, 531 (1960).

⁴ A. C. Butcher and J. M. McNamee, *Proc. Phys. Soc. (London)* **74**, 529 (1959).

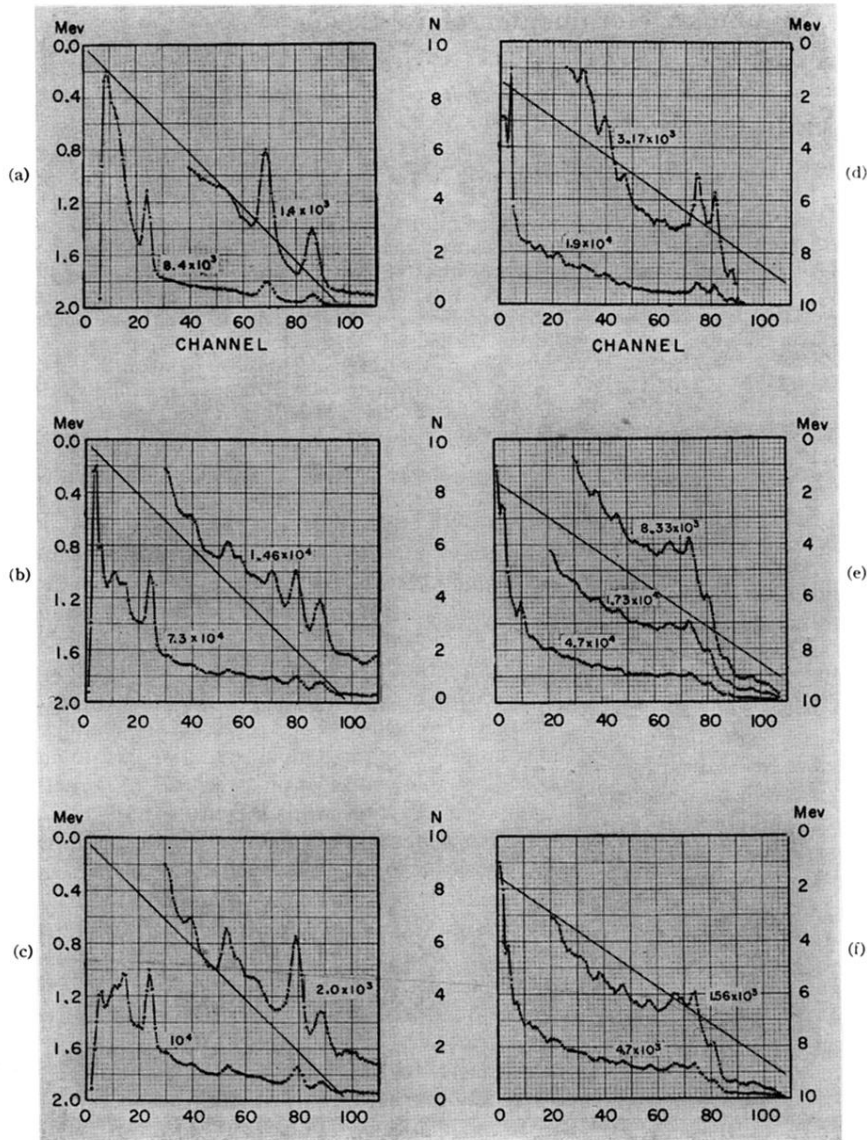


FIG. 1. (a) V^{52} and Al^{28} beta-decay gammas plus reactor background. (b) V^{51*} low-energy singles spectrum. (c) V^{51*} low-energy spectrum in total fast coincidence. (d) Al^{27} capture-gamma total singles spectrum. (e) V^{51*} total singles spectrum. (f) V^{51*} total spectrum in fast coincidence with 0.51 Mev. The number beside the plots is counts per unit of N scale.

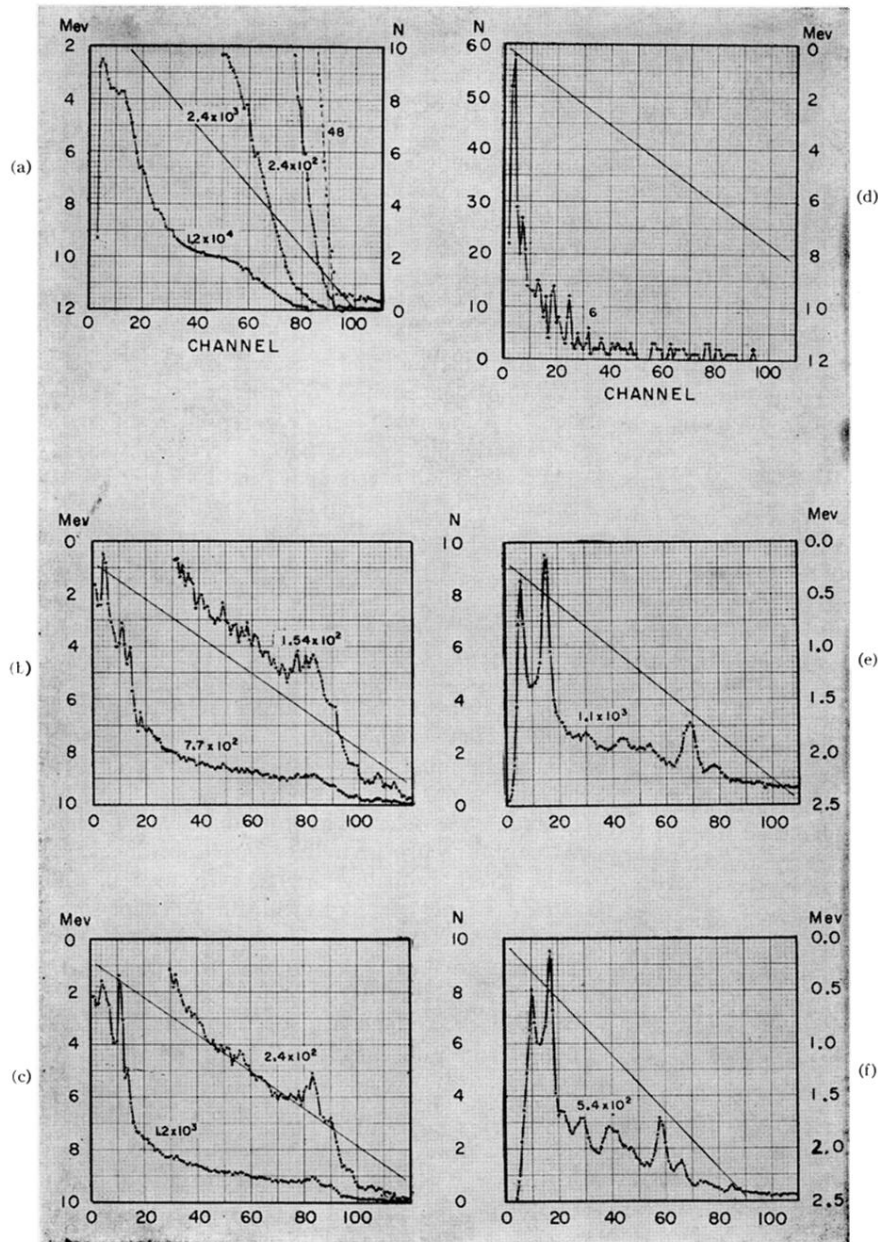


FIG. 2. (a) V^{51*} total sum spectrum in fast coincidence. (b) V^{51*} total spectrum in fast coincidence with 1.6 Mev. (c) V^{51*} total spectrum in fast coincidence with 1.8 Mev. (d) V^{51*} total spectrum in fast coincidence with 1.6 and 1.8 Mev. (e) V^{51*} low-energy spectrum in fast coincidence with 1.8 Mev. (f) V^{51*} low-energy spectrum in fast coincidence with 6.15 to 6.35 Mev. The number beside the plots is counts per units of N scale.

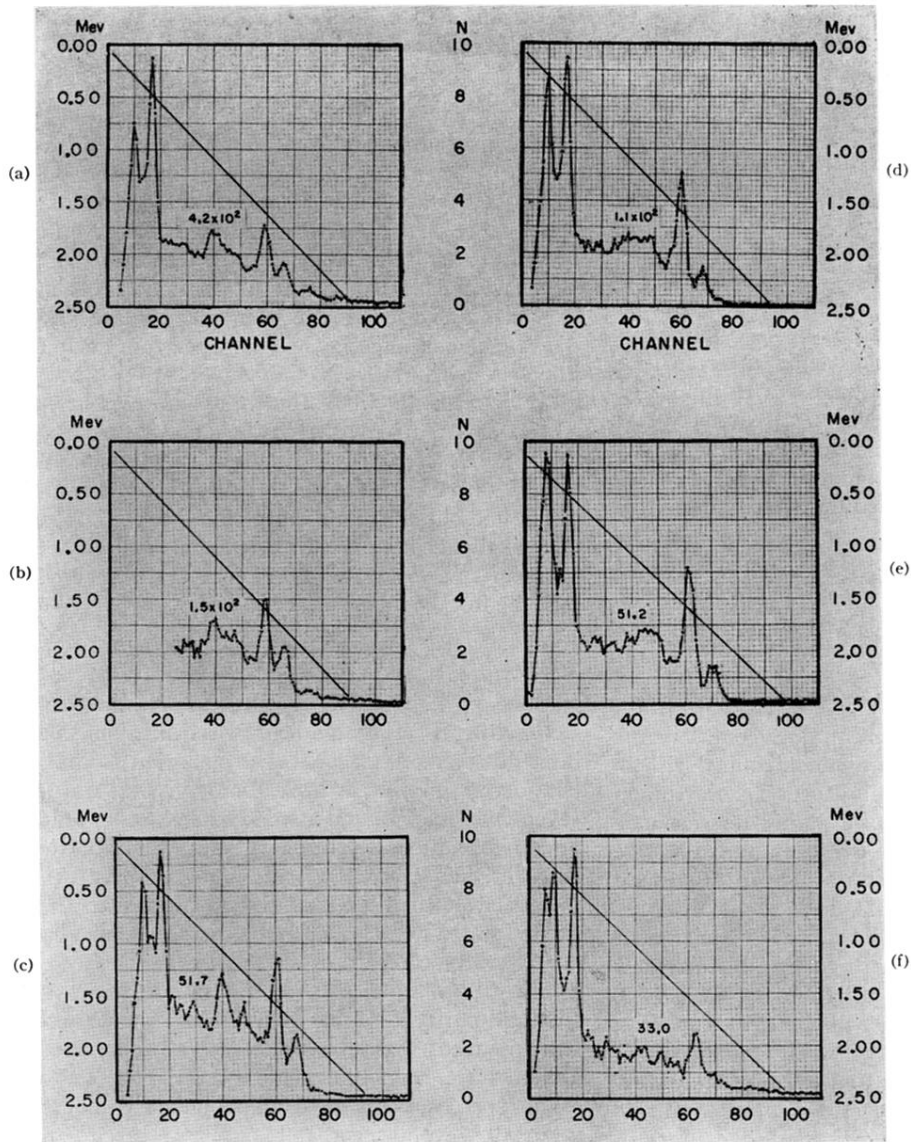


FIG. 3. (a) V^{51*} low-energy spectrum in fast coincidence with 6.65 to 6.85 Mev. (b) V^{51*} low-energy spectrum in fast coincidence with 7.15 to 7.35 Mev. (c) V^{51*} low-energy spectrum in fast coincidence with 7.6 to 7.8 Mev. (d) V^{51*} low-energy spectrum in fast coincidence with 8.25 to 8.35 Mev. (e) V^{51*} low-energy spectrum in fast coincidence with 8.7 to 8.9 Mev. (f) V^{51*} low-energy spectrum in fast coincidence with >9.3 Mev. The number beside the plots is counts per unit of N scale.

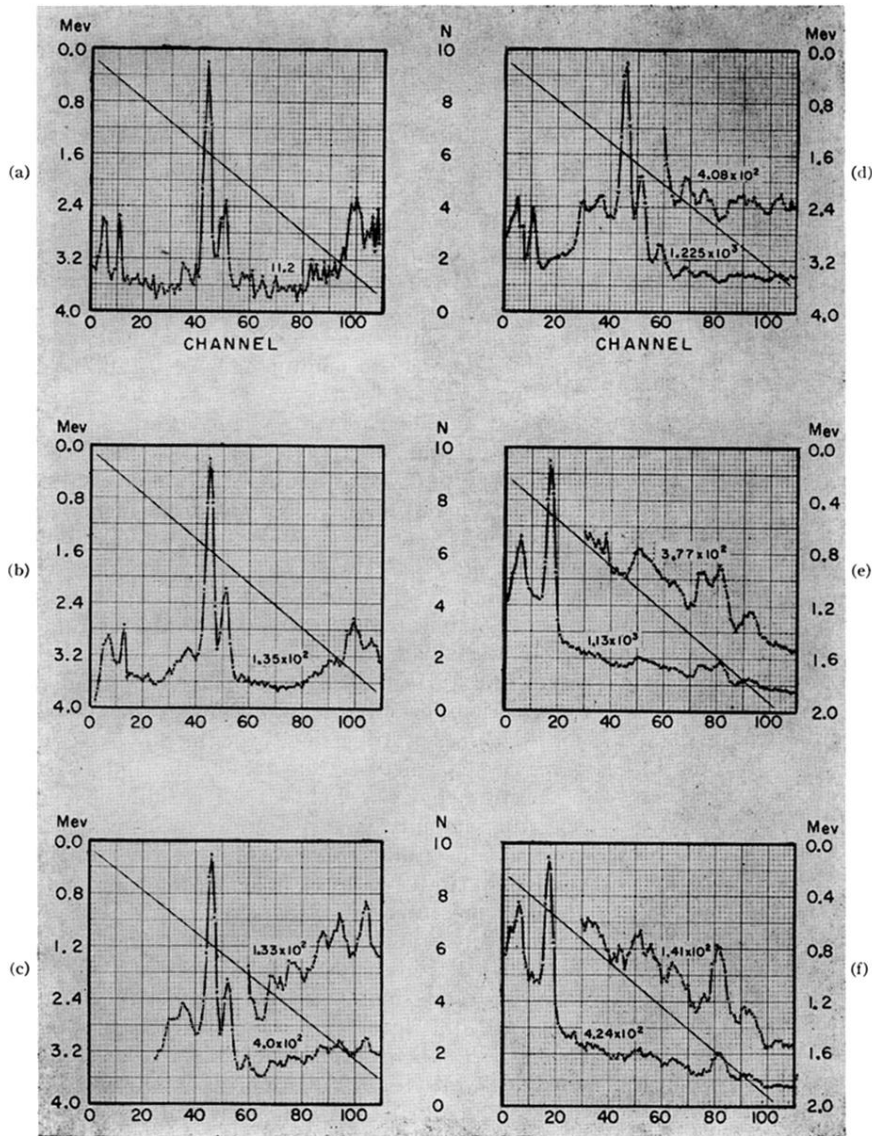


FIG. 4. (a) V^{51*} low-energy spectrum in fast coincidence and sum >10.5 Mev. (b) V^{51*} low-energy spectrum in fast coincidence and sum >10.0 Mev. (c) V^{51*} low-energy spectrum in fast coincidence and sum >9.15 Mev. (1.2 in the ordinate should read 1.6.) (d) V^{51*} low-energy spectrum in fast coincidence and sum >8.1 Mev. (e) V^{51*} low-energy spectrum in fast coincidence with 0.32 Mev. (f) V^{51*} low-energy spectrum in fast coincidence with 0.40 Mev. The number beside the plots is counts per unit of N scale.